

## Forced-Mixed Convection Transition of a Buoyant Axisymmetric Jet with Variable Properties

A. Abbassi<sup>1,2</sup>, and H. Ben Aissia<sup>1</sup>

**Abstract:** This paper describes the transition from forced to mixed convection in a jet flow with variable properties. The classical laminar layer analysis is extended by taking into account the dependence of physical properties on temperature. The related model relies on the assumption that the variations of Prandtl number and specific heat at constant pressure are sufficiently small to be neglected. A second-order finite-difference numerical method based on a staggered grid is used to analyze transition, hydrodynamic and heat transfer phenomena in the jet. The dimensionless control parameter,  $\Lambda = T_0/T_\infty$ , is limited to values less than 1. It is found that the variation of physical properties with temperature has a significant effect on jet flow velocity, whereas this dependence has an almost negligible influence on the expansion characteristics of the flow.

**Keywords:** Axisymmetric jet, forced convection regime, mixed convection regime, transition, variable properties.

### 1 Introduction

The relevance of jet flows to many potential industrial processes, for instance smoothing of solid, thermal insulation, film cooling, and meteorology attracts considerable attention, as witnessed by the numerous of experimental and numerical studies which have been made in this area [Schlichting (1979); Bickley (1937); Martynenko, Korovkin, and Sokovishin (1989); Yu, Lin, and Shih (1992); Aissia, Zaouali, and Golli (2002)]. Although most of these studies deal with the case of constant density, it should be pointed out, however, that most flows of practical interest are with variable density. Indeed, many physical processes can cause density variations like, for example, the existence of a strong gradient of temperature or a mixture of fluids with different densities. Also, density can be changed due

---

<sup>1</sup> Unit of Metrology and Energetic systems, UR11ES59, ENIM, Tunisia

<sup>2</sup> Corresponding Author: Email: ali\_persomail@yahoo.fr

to chemical reactions or by pressure changes related to high values of the Mach number (but such flows are outside the scope of the present paper).

In such a context, the study of hydrodynamic and heat transfer or transition phenomena from forced to mixed convection regimes is essential. For practical purposes, the knowledge of the relationship between small density changes, induced by temperature fluctuation, and other engineering aspects is very important. In the scientific literature, numerous analytical and numerical solutions exist for jet flow for various geometric configurations at diverse flow regimes. In fact, Schlichting, [Schlichting (1979)], for round jet, and Bickley, [Bickley (1937)], for two-dimensional jet, presented asymptotic solutions. These solutions were experimentally verified, respectively, by Andrade and Tsien, [Andrade and Tsien (1937)], for round jet, and Andrade, [Andrade (1939)], for a liquid-into-liquid two-dimensional jet. Also, Landau, [Landau and Lifshitz (1943)], presented an important solution of the complete Navier-Stokes equations using a round jet flow configuration. Yu, [Yu, Lin, and Shih (1992)] elaborated a rigorous solution for the two-dimensional buoyant jet valid for different flow regions, and Ben Aissia, [Aissia, Zaouali, and Golli (2002)] for an axisymmetric buoyant jet at Reynolds numbers in the range  $250 < Re_d < 1500$ . Likewise, Martynenko [Martynenko, Korovkin, and Sokovishin (1989)] published a detailed analytic study of self-similar class solutions of a laminar buoyant jet for many geometry configurations.

It should be noted that a laminar model has been used in this study, although flows are in most cases turbulent. There are two reasons behind this choice. First, a laminar model is easier in terms of computer implementation and, second, it is known that a turbulent jet can be mathematically treated in the same way as a laminar jet except that an empirical constant has to be determined experimentally [Schlichting (1979)]. In particular, on the basis of the Morkovin's hypothesis, the effect of mean density changes need to be included in the computation of a variable-density flow fields, while the effect of density fluctuations on the structure of turbulence is relatively small [Morkovin (1962)]. The way by which density changes influence the transition from an inertia-dominated flow to a buoyancy dominated one is connected to different mechanisms. Several studies have shown that density variations obtained by the mixing of two incompressible fluids can lead to an increase of turbulence in the intermediate region defined by  $0.69 < x/d < 1.66$ , [Panchapakesan and Lumley (1993)], where the dimensionless longitudinal distance  $X$  is given by  $x/d = Fr^{1/2}(\rho_j/\rho_\infty)^{1/4}X$ , [Chen and Rodi (1980)], and  $Fr$  is the Froude number defined by  $Fr = U_j^2 \rho_j (gd|\rho_\infty - \rho_j|)^{-1}$ . However, a heated jet for which density changes are produced by heating, gives the opposite effect [Chen and Rodi (1980); Chua and Antonia (1990); Peterson and Bayazitoglu (1992); Panchapakesan and Lumley (1993); Amielh, Djeridane, Anselmet, and Fulachier (1996)].

However, a heated jet for which density changes are produced by heating, is featured by the opposite effect [Chen and Rodi (1980); Chua and Antonia (1990); Peterson and Bayazitoglu (1992); Panchapakesan and Lumley (1993); Amielh, Djeridane, Anselmet, and Fulachier (1996)]. Despite the numerous papers that have been published in this area, some features, such as the variations of physical properties with temperature and related changes in the Prandtl number have not been fully explored. The main objectives of the study presented here are: (i) first testing a new mathematical model that takes into account the effects of small changes in physical properties with temperature (and related comparison with the conventional model based on the Boussinesq approximations), and (ii) second, giving a qualitative description of the hydrodynamics and heat transfer, in the near jet flow field. These objectives are achieved, by studying the effects of both, temperature-depending physical properties and Prandtl number on the dynamics of axial momentum and heat diffusion in both forced and mixed convection regimes.

## **2 Numerical analysis**

### **2.1 Hypothesis**

The jet flow is considered, to be two-dimensional, steady, incompressible, and laminar. It spreads upward, from a circular nozzle of diameter  $d = 2R$ , where  $R$  is the radius of its internal diameter, into a quiescent and unconfined medium at temperature  $T_\infty$ , filled with the same fluid. It is admitted that for large temperature differences, between jet and the surrounding medium, variations of physical properties with temperature may have significant impact on jet dynamics. Consequently, the mathematic model presented in this paper will take into account temperature dependency of physical properties. However, effects of viscosity and conductivity can be discussed separately of buoyancy since the latter is not explicitly influenced by these properties. For a given fluid, we assume that variations of Prandtl number and specific heat with temperature are sufficiently small to be neglected. The buoyancy effect is retained in the momentum equation, wherein density temperature depending obeys to Boussinesq approximations [Boussinesq (1903)], even for constant properties case [Kays and Crawford (1980)]. The Reynolds numbers  $Re = U_j d / \nu$  considered here, where  $d$  is the diameter of the nozzle,  $U_j$  is the initial mean velocity and  $\nu$  is the viscosity of the jet, are sufficiently high, remaining in the limit of small Mach number ( $M_0 \ll 1$ ), which allows the boundary layer model to be applied. The pressure is hydrostatically distributed throughout the jet flow. Also, viscous dissipation and change of temperature due to compression will be neglected in the energy equation.

### 2.2 Governing equations

Under the above assumptions the equations governing fluid motion, with boundary and initial conditions, in dimensionless form are given by

Continuity equation

$$\frac{\partial(\rho^*YU)}{\partial X} + \frac{\partial(\rho^*YV)}{\partial Y} = 0 \tag{1}$$

Momentum equation

$$\rho^*U \frac{\partial U}{\partial X} + \rho^*V \frac{\partial U}{\partial Y} = \frac{1}{Y} \frac{\partial}{\partial Y} (\mu^*Y \frac{\partial U}{\partial Y}) \pm \varepsilon \rho^* \theta \tag{2}$$

For the present analysis we assume that the specific heat  $C_p$  is constant, hence, the energy equation will be expressed in terms of temperature field,  $T$ , rather than enthalpy field,  $h$ . However, the relation between  $h$  and  $T$  is given by  $dh = C_p dT$ . Then, energy equation, using the dimensionless temperature variable, is written as follows

Energy equation

$$\rho^*U \frac{\partial \theta}{\partial X} + \rho^*V \frac{\partial \theta}{\partial Y} = \frac{1}{PrY} \frac{\partial}{\partial Y} (\lambda^*Y \frac{\partial \theta}{\partial Y}) \tag{3}$$

where  $\varepsilon$  in the momentum equation Eq. 2 takes values 0 and 1. For a non-buoyant jet flow ( $\varepsilon = 0$ ) the two conservation equations of momentum and energy are uncoupled. For the buoyant case,  $\varepsilon = 1$ , the sign + represents the case where the initial temperature ratio  $T_j/T_\infty > 1$  whereas the sign - represents the case where the initial temperature ratio  $T_j/T_\infty < 1$ . These equations are written in cylindrical co-ordinates such as the origin of the axes is in the middle of the nozzle exit.

We used here the following dimensionless variables

$$\begin{aligned} (X, Y) &= \left( \frac{x}{dGr}, \frac{y}{d} \right), (U, V) = \left( \frac{ud}{vGr}, \frac{vd}{v} \right), \\ \theta &= \frac{T - T_\infty}{T_j - T_\infty}, \rho^* = \frac{\rho}{\rho_\infty}, \mu^* = \frac{\mu}{\mu_\infty}, \lambda^* = \frac{\lambda}{\lambda_\infty} \end{aligned} \tag{4}$$

where  $\mathbf{X} = (X, Y)$  is the dimensionless coordinates vector,  $\mathbf{U} = (U, V)$  is the dimensionless fluid velocity vector,  $\theta$  is the dimensionless temperature field,  $d$  is the

diameter of the nozzle,  $T_j$  is the temperature of the jet fluid,  $T_\infty$  is the temperature of the surrounding medium,  $\rho_\infty, \nu_\infty, \lambda_\infty$  are, respectively, the density, the viscosity, and the thermal conductivity of the surrounding medium,  $Gr$  is the Grashoff number defined by  $Gr = g\beta (T_j - T_\infty) d^3 / \nu^2$  in which,  $g$  is the gravitational acceleration,  $\beta$  is the thermal dilatation coefficient, and  $\nu$  is the viscosity of the jet fluid.

The dimensionless boundary conditions are given by

$$\begin{aligned}
 Y = 0; \quad \frac{\partial U}{\partial Y} = 0, \quad \frac{\partial \theta}{\partial Y} = 0, \quad V = 0 \\
 Y \rightarrow \infty; \quad U \rightarrow 0, \quad \theta = 0
 \end{aligned}
 \tag{5}$$

and the dimensionless initial conditions, at the nozzle exit, are given by [Aissia, Zaouali, and Golli (2002)]

$$X = 0; V = 0 \text{ and : } \left\{ \begin{array}{l} * 0 < Y < 0.5 \\ \text{Uniform profile :} \\ U = 1; \theta = 1 \\ \text{Parabolic profile :} \\ U = (3.)^{0.5}(1 - 4Y^2); \\ \theta = (3.)^{0.5}(1 - 4Y^2) \\ * Y > 0.5 \\ U = 0; \theta = 0. \end{array} \right.
 \tag{6}$$

The constants which appear in velocity and temperature profiles at the nozzle exit are given so that constraints of integration, expressing the momentum and energy conservation along the jet axis, are satisfied [Martyntenko, Korovkin, and Sokovishin (1989)]. In addition to these initial and boundary conditions integral conditions hold. As the mass flow rate,  $Q_0$ , must be the same for constant and variable properties from  $Q_0 = 2\pi C_p \int_0^\infty \rho u \Delta T y dy$  where the second integral condition expressing conservation of momentum along  $X$ -direction is given by  $K_0/2\pi = \int_0^\infty \rho u^2 y dy$ .

### **2.3 Physical properties**

In this section we are going to present the property-ratio method used to establish temperature depending of physical properties for small heating rates. This method represents a rational asymptotic approximation for small heating rates which are be improved by higher order terms. All physical properties involved in the present investigation ( $\rho, \mu$  and  $\lambda$ ) are more or less pressure and temperature depending. To quantify this behaviour, property-ratio method consists in expanding these property

functions as Taylor series at the reference state, one finally comes out with correction factors for the physical properties. The physical properties,  $\varphi = (\rho, \mu, \lambda)$ , then reads, where  $r$  signify reference state, which is taken at ambient ( $\infty$ )

$$\varphi = \varphi_r + \left(\frac{\partial \varphi}{\partial T}\right)_r (T - T_r) + \left(\frac{\partial \varphi}{\partial P}\right)_r (P - P_r) + \dots \tag{7}$$

which leads to the following equations in dimensionless form

$$\varphi^* = 1 + K_{\varphi^*} \theta + K'_{\varphi^*} P + \dots \tag{8}$$

where  $K_{\varphi} = \left(\frac{T}{\varphi} \frac{\partial \varphi}{\partial T}\right)_r$  and  $K'_{\varphi} = \frac{\rho_r U_j^2}{P_r} \left(\frac{P}{\varphi} \frac{\partial \varphi}{\partial P}\right)_r$  with  $\varphi$  (here  $\rho, \mu$  and  $\lambda$ ). Here, the two parameters  $K_{\varphi}$  and  $K'_{\varphi}$  are dimensionless numbers characterising the fluid like the Prandtl number does. Through the use of these two numbers  $K_{\varphi}$  and  $K'_{\varphi}$  one can easily select the important dependencies of physical properties with temperature and pressure.

Table 1: Variation of physical properties with temperature and pressure [Gersten (1983)]

	$K_{\rho}$	$K_{\mu}$	$K_{\lambda}$	$K'_{\rho}$	$K'_{\mu}$	$K'_{\lambda}$
Air	-1.01	0.70	0.83	1.0	$8.5 \times 10^{-3}$	$1.3 \times 10^{-3}$
Water	-0.06	-7.37	0.75	$5.4 \times 10^{-5}$	$1.0 \times 10^{-3}$	$1.5 \times 10^{-4}$

In Tab. 1 the values for air and water are listed. It should be noted that the pressure dependence is almost always negligible as  $K'_{\varphi}$  is extremely small (and so  $\varphi$  is nearly constant with respect to  $p$ ). Only gases have considerable values of  $K'_{\varphi}$ . However, for gases  $(\partial P / \partial \rho)_{T_r} = a_r^2 / \gamma$  (where  $\gamma = C_p / C_v$ ), with  $a_r$  being the local speed of sound, and  $K'_{\rho}$  is  $K'_{\rho} = \gamma M_r^2$  [Landau and Lifshitz (1943)]. Now, we restrain ourselves to small Mach numbers ( $M \rightarrow 0$ , asymptotically) and so are left over with the physical properties being dependent on temperature only. As a result of this, for small heat transfer rates and small temperature differences, the linear approximation to the function  $\varphi(T)$  according to equation Eq. 8 may be sufficient. If higher accuracy is desired an extension of what is present here as linear theory is straightforward. Then, in the Taylor series expansion, equation Eq. 7, higher order terms, neglected here, have to be taken into account. For relatively small changes

of physical properties like density, viscosity and thermal conductivity with temperature, the property ratio is made by fitting the property values between the desired temperature limits, using the power-law approximations Svehla [Svehla (1962)]. These equations are expressed as follows

$$\begin{aligned}
 \text{Density} & : \rho^* = [1 + \theta(\Lambda - 1)]^\sigma \\
 \text{Viscosity} & : \mu^* = [1 + \theta(\Lambda - 1)]^\kappa \\
 \text{Conductivity} & : \lambda^* = [1 + \theta(\Lambda - 1)]^\gamma
 \end{aligned} \tag{9}$$

Where the three constants are chosen to be equal  $\sigma = -1$ ,  $\kappa = 0.71$  and  $\gamma = 0.85$ , respectively. These powers are also consistent with the kinetic theory of gases [Kennard (1938)], [Hirschfelder, Curtiss, and Bird (1954)], and are accurate descriptions for the properties of air in the 600 to 1600K range and [Brown and Donoughe (1951)] and [Kays and Crawford (1980)]. The final result is universal in the sense that it holds for all fluids, for example liquid metals, liquids, gases and oils. There is no need to distinguish between liquids and gases as usually done when the property ratio method is applied, see for example [Kays and Perkins (1973)].

#### 2.4 Computational details

Noting that in the present investigation only positive effect of the buoyancy term on the momentum equation will be considered. Thus, the plus sign represents the case of the cold fluid downward which corresponds to the initial temperature ratio  $\Lambda$  less than 1, for a value greater than 1, corresponds to a hot fluid ejected upward Fig. 1. Consequently, the momentum and the energy conservation equations Eq. 2 and Eq. 3 are coupled and highly nonlinear in nature.

A two dimensional staggered mesh is superimposed in the flow field shown in Fig. 1. In the  $x$ -direction the index  $i$  varies from 0 at the center of the nozzle to  $I_{max}$  at the end of the numerical domain by increment step  $i + 1$  (*i.e.*,  $X + \Delta X$ ). Index  $j$  varies from 0 at the center jet to  $J_{max}$  at the edge of boundary layer by increment step  $j + 1$  (*i.e.*,  $Y + \Delta Y$ ). Momentum and energy equations (Eq. 2 and Eq. 3) are discretized by taking central difference along  $X$  direction and  $Y$  direction with nodes  $(i + 1/2, j)$ . The truncation error of these equations is  $O(\Delta X^2, \Delta Y^2)$ . This gives a second order accurate solution in  $X$  and  $Y$  for the streamwise velocity component  $U$  and the dimensionless temperature  $\theta$ , respectively. The continuity equation (Eq. 1) is then discretized by taking central scheme for both  $X$  and  $Y$  directions with nodes  $(i + 1/2, j + 1/2)$ . The truncation error of this equation is  $O(\Delta X^2, \Delta Y^2)$ . This gives also a second order accurate solution for the transverse

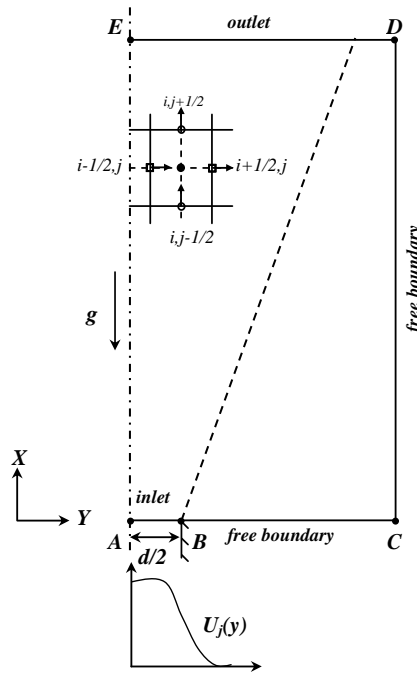


Figure 1: Geometry of the problem (jet half-space) and staggered cell definition

velocity component  $V$ . Properties  $\rho^*$ ,  $\mu^*$ , and  $\lambda^*$  are evaluated by using Eq. 9 for the converged temperature.

The discretized forms of governing equations (continuity,  $x$ -momentum and energy equations) used for the present analysis is similar to the one presented elsewhere by [Dalbert, Penot, and Peube (1981)]. It was adopted for reasons of numerical stability compared with regular mesh. Solution of the governing equations are obtained by a marching technique from the point  $X = 0$ . First, momentum equation (Eq. 2) is solved to get fresh values of  $U$ , using initial conditions of velocity and temperature (Eq. 6). Second, the continuity equation is solved by substituting the obtained values of  $U$  from momentum equation (Eq. 1) to get the new values of transverse velocity  $V$ . Then temperature field  $\theta$  is obtained by injection of the two velocity components  $U$  and  $V$  in energy equation (Eq. 3). Finally properties  $\rho^*$ ,  $\mu^*$  and  $\lambda^*$  are evaluated from fresh values of  $\theta$ , by using (Eq. 9). Solution of the tridiagonal algebraic system is obtained by using Thomas algorithm [Fletcher (1991)]. The iterative solution procedure consists of solving momentum, continuity, energy and property equations in that order repeatedly until convergence is obtained. The solution is converged when the relative changes of the streamwise velocity compo-

nent  $U$  between two successive iterations is lower than  $10^{-5}$  for each node of the calculation domain. The converged variables ( $U$ ,  $V$  and  $\theta$ ) obtained from  $j = 0$  to  $j = J_{max}$  at a particular  $i$  location is used to get values of variables for next location, (*i.e.*,  $i + 1$ ) during marching procedure. Marching procedure is continued until the boundary layer development is almost complete ( $J_{max}$  is reached). Thus, the asymptotic nature of the boundary layer edge ( $Y \rightarrow \infty$ ) which is visible in the results obtained by the procedure followed. Grid size in the  $X$  direction ( $\Delta X$ ) is increased as we march along the  $X$  direction from an initial  $\Delta X$  of  $1.10^{-4}$  near to the jet exit until a maximum value  $10^{-2}$  from  $X > 12$  to be able to go further downstream in the jet. Grid step size in the  $Y$  direction  $\Delta Y$  is taken constant of  $10^{-3}$ . A sufficient grid point,  $N$ , is taken in that direction to ensure the boundary condition  $Y \rightarrow \infty$ . It is noted that the same code is used for the case with constant physical properties with minor changes.

### 3 Results and discussions

The analysis of results issued from numerical integration of governing equations for a free buoyant round jet with variable physical properties, covers the entire buoyancy region. The effects of Prandtl number on hydrodynamic and heat transfer of the jet are illustrated by computing the streamwise velocity component  $U$ , the transverse velocity component  $V$ , the modified centerline velocity  $U_{cm}$ , the modified centerline temperature  $\theta_{cm}$ , the dimensionless dynamical half-width  $Y_u^*$ , which is defined by the transverse location at which  $U = U(Y = 0)/2$ , and the dimensionless thermal half-width  $Y_\theta^*$ , which is defined by the transverse location at which  $\theta = \theta(Y = 0)/2$ . The range of the governing parameters (Richardson number defined by  $Ri = Gr/Re^2$ , Reynolds number  $Re = U_j d/\nu$ , where  $U_j$  is the initial mean velocity at the nozzle exit, and initial temperature ratio between the jet and the surrounding medium  $\Lambda$ ) used in the present investigation  $1.67 \times 10^{-6} < Ri < 2.5$ , from forced convection regime where viscous forces are dominant compared to the buoyant one, to the mixed convection region,  $Re = 586,830$  which used in a previous study [Yassine, Aissia, Kechiche, Jay, and Schon (2004)] and  $0.15 < \Lambda < 0.9$ . Results are compared with results of constant physical properties model.

#### 3.1 Velocity and temperature profiles

In this section, results are presented only for the uniform initial velocity profile at several Prandtl numbers and an assisting effect of the buoyancy corresponding to the range temperature ratio equal to  $0 < \Lambda < 1$ .

The influence of Prandtl number on the evolution of the streamwise velocity component  $U$ , at different longitudinal locations  $X$  measured from the nozzle exit, is

given by Fig. 2 and compared with results obtained by the constant physical properties model. Three streamwise distances  $X$  are chosen to be equal to 0.15, 2.5 and 27.5 which corresponds to different regions of the jet development: inertial region, potential core and plume region, respectively. In the vicinity of the jet exit, inertial region, corresponding to the streamwise distance  $X = 0.15$ , the transverse variation of the streamwise velocity component  $U$  presents two different zones, the first one corresponds to the center jet region ( $Y = 0$ ), in which the velocity profiles are independent to the Prandtl number. For spanwise distances  $Y$  far from the center jet the velocity profile becomes flatter for decreasing Prandtl numbers which define the second zone. In the potential core region corresponds to the streamwise distance  $X = 2.5$  as shown in Fig. 2b, the streamwise velocity component  $U$  also presents two distinct zones. In the first zone which corresponds to the spanwise distance  $Y = 0$ , the velocity profile keep a constant value independent to the Prandtl number, with a length smaller than that obtained in the inertial region.

In the plume region, corresponding to the streamwise distance  $X = 27.5$ , jet flow streamwise velocity component  $U$  profiles are represented in Fig. 2c. It should be noted that the first zone characterized by a constant value disappears completely with a significant increase, proportionally to the Prandtl number, in the centerline velocity  $U_c$  of the jet, where  $U_c$  is the centerline velocity defined for  $Y = 0$ . In addition, Fig. 2c shows that the velocity profiles become more flatted which proves that the expansion of the jet becomes less important. This behaviour will be analyzed in the following sections.

As in Ben Aissia [Aissia, Zaouali, and Golli (2002)], jet expansion, in the spanwise direction  $Y$ , will be analyzed by means of two quantities, the dynamical half-width  $Y_u^*$  and the thermal half-width  $Y_\theta^*$ , for various Prandtl numbers, as shown in Fig. 3. The axial evolution of these parameters attests, for the entire range of Prandtl numbers used in the present analysis, the existence of three regions with different jet behaviour. It is obvious that the spanwise jet spreading is more important for decreasing Prandtl numbers. This phenomenon is characterized by a negative value of the transverse velocity component  $V$ . In fact, the spreading jet is caused especially by the augmentation of the rate of the surrounding medium entering in the jet flow. This behaviour will be explained, by analysing the transverse velocity component  $V$ , the limit transverse velocity  $V_{lim}$ , the dynamical core length  $X_u$  and thermal core length  $X_\theta$  as a function of the two parameters  $\Lambda$  and the Prandtl number  $Pr$ , in the next paragraph.

The transverse velocity component  $V$  distributions, for  $Re = 586$  and for several Prandtl numbers  $Pr = 0.71, 2.00$  and  $10.00$ , at three streamwise locations measured from the nozzle exit  $X = 0.15$  (inertial region),  $X = 2.5$  (potential core region) and  $X = 27.5$  (plume region), respectively are shown in Fig. 4 and compared

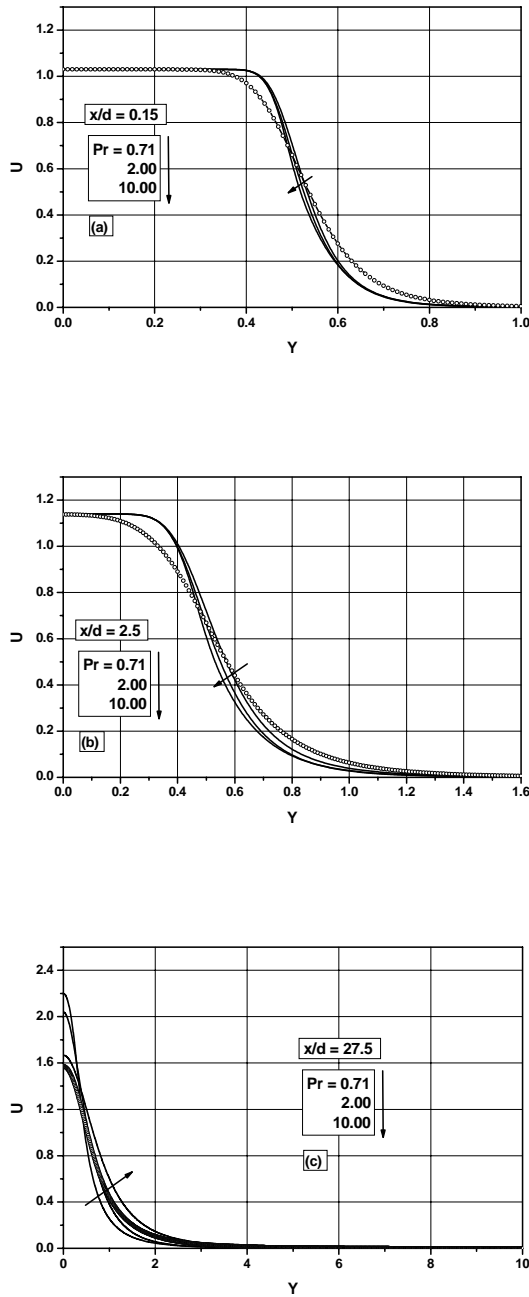


Figure 2: Evolution of the streamwise velocity component of the jet influenced by Prandtl number and compared with results obtained by the constant physical properties model, symbol line ( $\circ$ ). (a) jet zone; (b) transition zone and (c) plume zone. (initial uniform profile,  $Ri = 0.1$  and  $\Lambda = 0.5$ ).

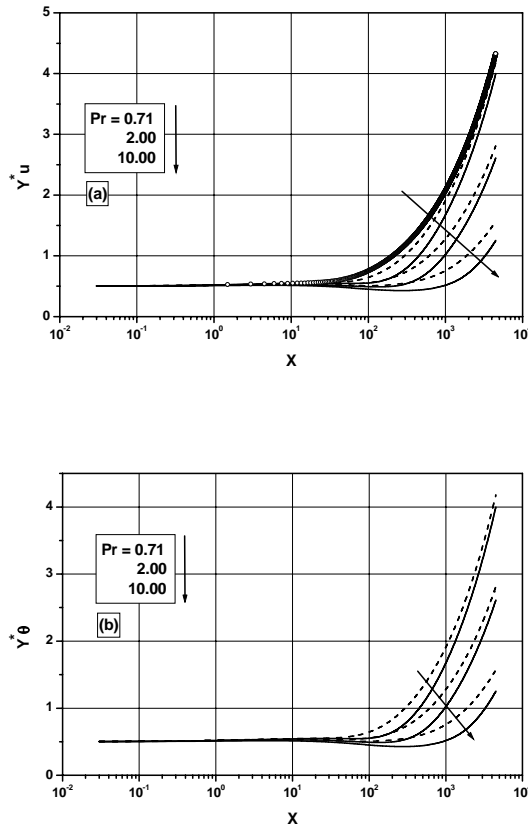


Figure 3: Effect of Prandtl number. (a) Dynamical half-width compared with that of constant physical properties, symbol line ( $\circ$ ). (b) Thermal half-width. (solid line:  $\Lambda = 0.50$ , dashed line:  $\Lambda = 0.75$   $Ri = 0.01$ ).

with results of the constant physical properties model. In the initial region close to the nozzle exit, for streamwise distance  $X = 0.15$  as shown in Fig. 4a, the Prandtl number have no effect along the center of the jet, at  $Y = 0$ . In this zone the transverse velocity component  $V$  have a negative value magnitude (inward) due to the increase of the streamwise velocity component  $U$  at the center jet, independently to the Prandtl number. In fact, it can be seen that the transverse velocity component  $V$  reaches a maximum near to the edge of the nozzle exit ( $Y \approx 0.5$ ) and decreases again. Far from the jet center this component increases while remaining negative. It is worth to note that the increase of the transverse velocity is inversely proportional to the Prandtl number. The same observations remain valid in the intermediary region (transition region until the end of the potential core) as shown in Fig. 4b defined at the streamwise location  $X = 2.5$ . However, it should be noted that in the third region defined at  $X = 27.5$  from the nozzle exit, as shown in Fig. 4c, the velocity component  $V$  haven't a negative part near the center jet and this can be explained by the increase in the rate of the surrounding fluid entering in the jet flow, which explains jet spreading in the spanwise direction  $Y$  as shown by the evolution of the axial growth of the dynamical half-width  $Y_u^*$ .

As one of the important characteristics of jet flow is entrainment, Fig. 5 shows the evolution of the limit transverse velocity  $V_{lim}$  (for  $Y \rightarrow \infty$ ) as a function of the initial temperature ratio  $\Lambda$ . It is significant to note, on the one hand the amount of fluid from the surrounding medium added to the jet, by entrainment phenomenon, decreases with streamwise distance  $X$ . On the other hand, in the first region, before  $X \approx 10$ , the entrainment decreases rapidly according to the streamwise distance  $X$ . After this location, which is the plume region, the entrainment rate is quite small. In addition, the figure also suggests that an increase in the initial temperature ratio generates a more significant entrainment of the external fluid. As a consequence of the entrainment, which increases for increasing  $\Lambda$ , is the expansion of the jet (spread) that defines another important characteristic of the jet which described by the dynamical half-width  $Y_u^*$  instead of the momentum thickness [Aissia, Zaouali, and Golli (2002)]. In Fig. 6, we represent the evolution of the dynamical core length  $X_u$ , where  $X_u$  is defined by the longitudinal location at which  $u = 0.99U_j$ , and thermal core length  $X_\theta$ , where  $X_\theta$  is defined by the longitudinal location at which  $T - T_\infty = 0.99(T_j - T_\infty)$ , as a function of the initial temperature ratio  $\Lambda$ . We notice that these two characteristics,  $X_u$  and  $X_\theta$ , varies linearly according to  $\Lambda$  and can be predicted by the proposed correlation equations Eq. 10 and Eq. 11, respectively.

For the dynamical core length  $X_u$  we propose the correlation :

$$\log X_u = -1.763 \log \Lambda + 0.744 \quad (10)$$

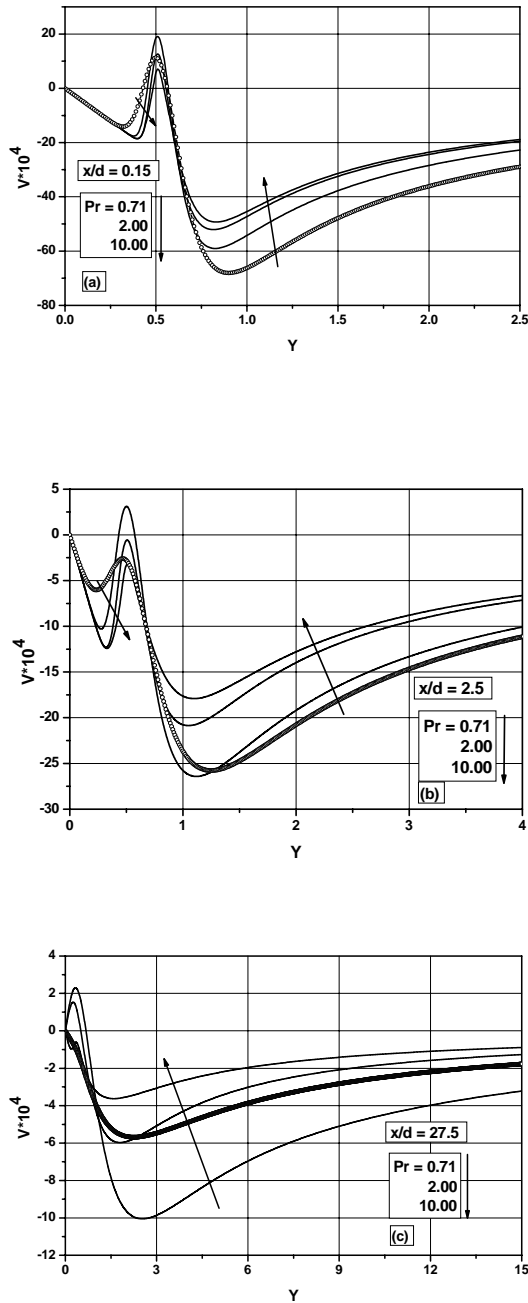


Figure 4: Evolution of the transverse velocity component of the jet influenced by Prandtl number and compared with that of constant physical properties, symbol line ( $\circ$ ). (a) jet zone; (b) transition zone and (c) plume zone. (initial uniform profile,  $Ri = 0.01$  and  $\Lambda = 0.50$ )

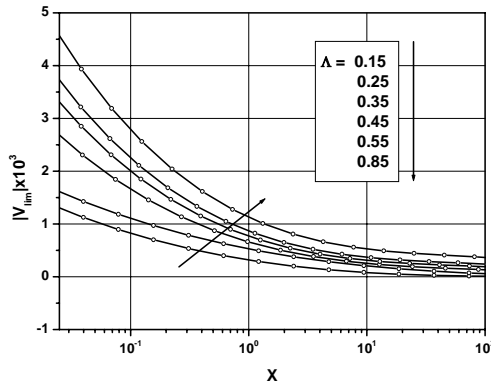


Figure 5: Evolution of the limit transverse velocity of the jet influenced by the parameter  $\Lambda$  (forced convection regime). ( $Pr = 0.71$ ,  $Ri = 1.67 \times 10^{-6}$  and  $Re = 586$ .)

For the thermal core length  $X_\theta$  we propose the correlation :

$$\log X_\theta = -1.807 \log \Lambda + 0.602 \tag{11}$$

In this paragraph, we are interested to the influence of the Prandtl number on the evolution of the temperature field. The analysis is conducted at three streamwise locations  $X = 0.15$  (inertial region),  $X = 2.5$  (potential core) and  $X = 27.5$  (plume region) as depicted in Fig. 7. To highlight the effect of density variation on jet, results are compared with those obtained by the constant physical properties model. However, we notice that the analysis of the temperature distribution field is more complicated than that of velocity field. In fact, temperature evolution is appeared as a result of competition between two processes having opposite effects, that will be discussed in the next paragraph. At streamwise distance  $X = 0.15$ , corresponding to the inertial region, we notice that the temperature keep a constant value, in the zone close to the jet center, as shown in Fig. 7a and Fig. 7b. On the one hand, in this zone we also remark that temperature evolution is independent to the Prandtl number. On the other hand, at streamwise location equal to  $X = 27.5$ , Fig. 7c, we note that the temperature field, at the jet center  $Y = 0$ , increases with increased Prandtl numbers. It should be noted that, the main effect of variable physical properties, which is still true for all jet characteristics ( $U$ ,  $V$  and  $\theta$ ), is that the transverse velocity component, for instance, have values to be more negative compared to those obtained by the constant properties model.

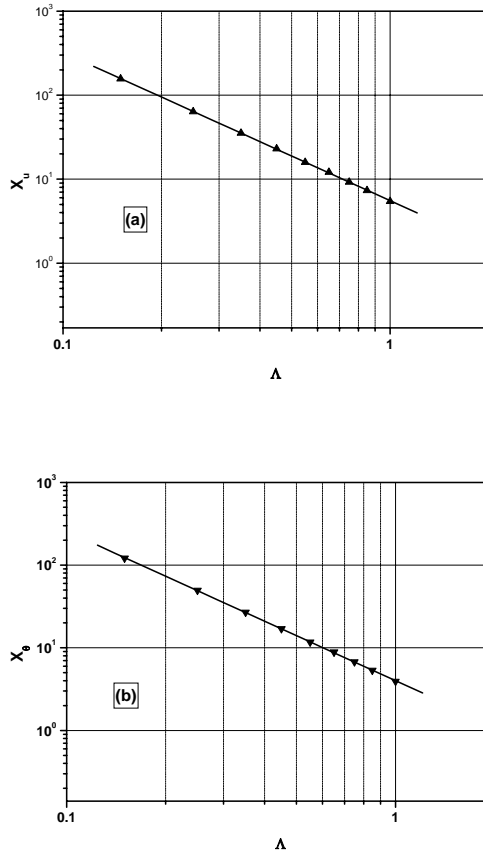


Figure 6: Effect of the parameter  $\Lambda$  (forced convection regime). (a) Dynamical core length  $X_u$ . (b) Thermal core length  $X_\theta$ . ( $Pr = 0.71$ ,  $Ri = 1.67 \times 10^{-6}$  and  $Re = 586$ .)

To study jet flow transition from forced convection regime to mixed convection regime, we presented in this paragraph the buoyancy magnitude effect on the dynamical half-width  $Y_u^*$  and the thermal half-width  $Y_\theta^*$  evolution as function of Richardson number which measure the magnitude of buoyancy compared to the inertia forces, as shown in Fig. 8. In Fig. 9, we represent the dynamical half-width  $Y_u^*$  and the thermal half-width  $Y_\theta^*$  distributions as function of the initial temperature ratio  $\Lambda$ . A correlation for the streamwise transition distance  $X_p^*$  from inertial region to the plume region is given for all the convection regimes, ie, for Richardson num-

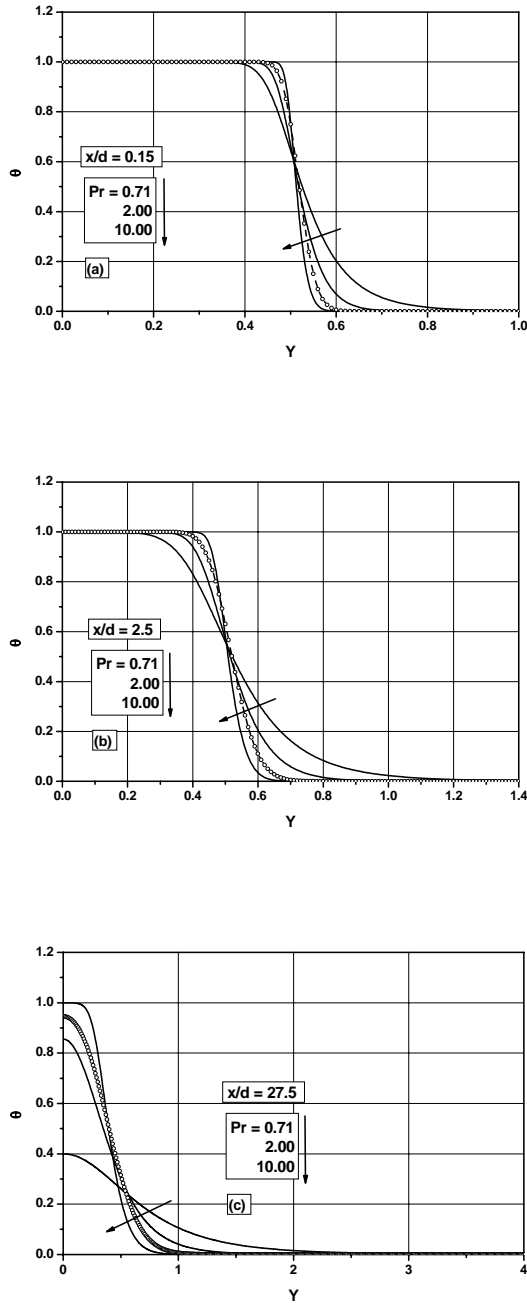


Figure 7: Evolution of the temperature ( $\theta$ ) of the jet influenced by Prandtl number and compared with that of constant physical properties, symbol line ( $\circ$ ). (a) jet zone; (b) transition zone and (c) plume zone. (initial uniform profile,  $Ri = 0.01$  and  $\Lambda = 0.50$ )

ber in the range  $5 \times 10^{-2} < Ri < 0.5$  and for initial temperature ratio in the range  $0.15 < \Lambda < .95$  as shown in Fig. 10.

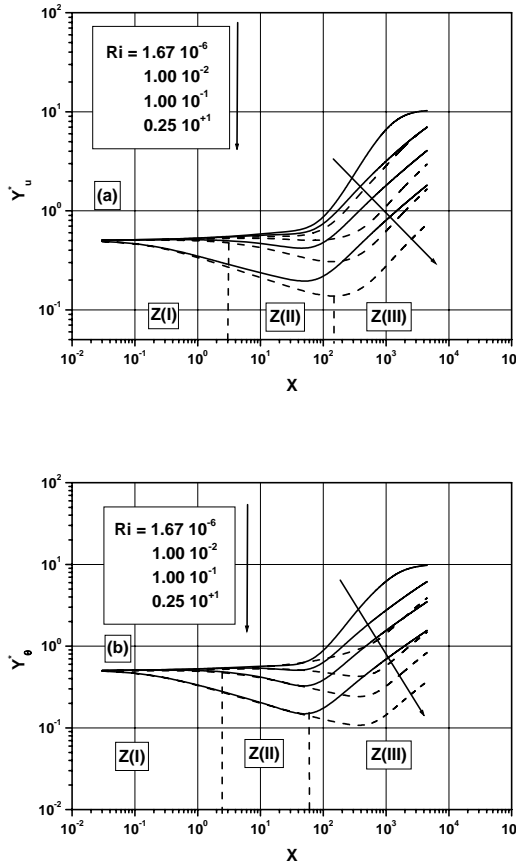


Figure 8: (a) Dynamical half width  $Y_u^*$ . (b) Thermal half width  $Y_\theta^*$ . Z(I): jet zone; Z(II): transition zone and Z(III): plume zone. (initial uniform profile, solid line:  $Pr = 0.71$ , dashed line:  $Pr = 6.7$   $Re = 586$ . and  $\Lambda = 0.50$ )

Fig. 8, shows that the buoyancy term taken in the  $x$ -momentum equation Eq. 2, using Boussinesq approximations to describe small density variations with temperature, have different effects on dynamical half-width  $Y_u^*$  and thermal half-width  $Y_\theta^*$  according to the streamwise distance  $X$  measured from the nozzle exit. Initially, for small values of  $X$ , close to the nozzle,  $0 < X \leq 10$ , we notice that buoyancy has a negligible effect on both hydrodynamic and thermal parameters. In that zone,

jet behaves like a pure momentum source identically to an isothermal jet flow. It should be noted that Prandtl number haven't any effect on these parameters. This zone is called: jet zone in which the flow is governed mainly by inertial forces. In the intermediate section between  $X \approx 10$  and  $X \approx 100$ , we notice a small decreases of both  $Y_u^*$  and  $Y_\theta^*$  in the streamwise direction  $X$ . This behavior is more acute for higher Prandtl numbers. Indeed, this decrease can be explained by an increase in the buoyancy forces which become in the same magnitude with inertial forces. This zone is called transition (or intermediary region) or mixed convection region. Both

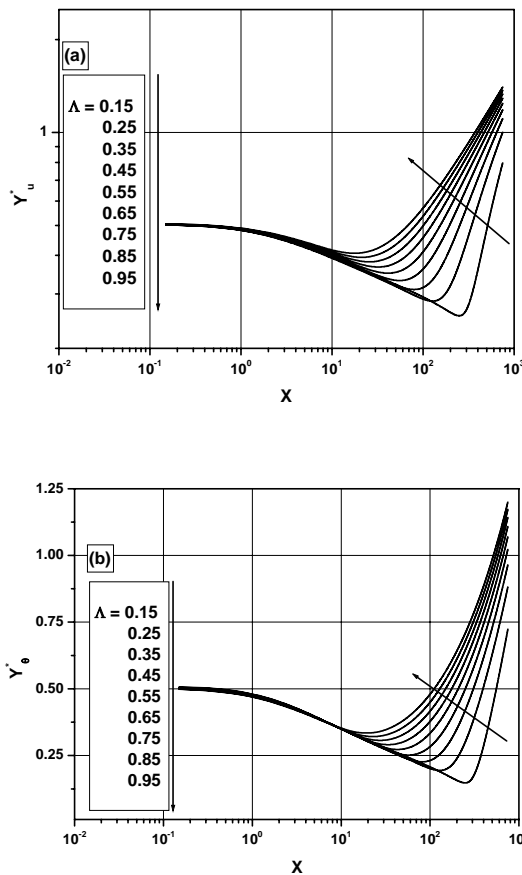


Figure 9: Effect of the parameter  $\Lambda$  on dynamical and thermal half-widths (mixed convection regime). (a) Dynamical half-width  $Y_u^*$ . (b) Thermal half-width  $Y_\theta^*$ . ( $Pr = 0.71$ ,  $Ri = 0.25$ ) and  $Re = 586..$

$Y_u^*$  and  $Y_\theta^*$  parameters reaches a minimum value in the  $X$ -direction after which they increase rapidly. The minimum value attained by these two parameters depend on both Richardson and Prandtl numbers. This behavior is the same for both  $Y_u^*$  and  $Y_\theta^*$  as demonstrate Fig. 8a and Fig. 8b, respectively. Also, the initial temperature ratio  $\Lambda$  effect on these parameters is discussed as shown in Fig. 9. The same observations remain valid as previously described and we notice the existence of three distinct zones along the streamwise distance  $X$  measured from the jet exit. In Fig. 10, we represent the streamwise location  $X_p^*$  evolution from which the panache region starts as initial temperature ratio  $\Lambda$  and of Richardson number  $Ri$  functions as shown in Fig. 10a, and Fig. 10b, respectively. This behavior can be predicted by the proposed correlation equations Eq. 12 and Eq. 13 giving the  $X_p^*$  transition parameter.

$$\log X_p^* = 0.1086 \log Ri + 1.384 \quad (12)$$

and,

$$X_p^* = \alpha(Ri) Ri^{-\frac{1}{2}} \Lambda^{-\frac{5}{4}} \quad (13)$$

where  $\alpha(Ri) = 22.1 Ri^{0.4917}$ .

In conclusion, taking into consideration the analysis made in the first part of the present study, variable density jet behaviour can be divided into two distinct regimes (or regions) depending on the three parameters  $Ri$ ,  $Pr$  and  $\Lambda$ . According to the first parameter, Richardson number, the first regime is called forced convection regime, defined for small values of  $Ri$ , in which hydrodynamic and heat transfer is mainly governed by inertia forces contrariwise the buoyancy effect appears only at very high distances  $X$  measured from the nozzle exit. The second regime is called mixed convection regime, characterized by high Richardson values, in which buoyancy effect dominate. In the second part of the present paper we are going to analyse each one separately.

### 3.2 Forced convection regime

#### 3.2.1 Centerline velocity and temperature

In this part we presented the hydrodynamic and thermal characteristics of the jet in forced convection regime. In that regime, momentum and heat transfer are mainly controlled by inertia forces. For this reason we take small value of Richardson number  $Ri = 5 \times 10^{-4}$ . The analysis is focused in studying Prandtl number  $Pr$  and initial temperature ratio  $\Lambda$  effects on jet dynamic. In all simulations presented

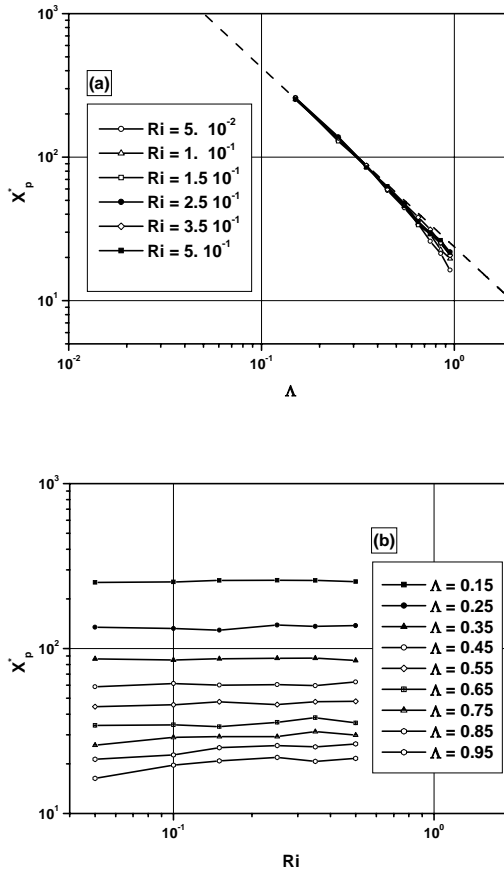


Figure 10: (a) Evolution of the panache distance according to the parameter  $\Lambda$ , from forced convection regime  $Ri = 5 \cdot 10^{-2}$  to mixed convection regime  $Ri = 0.5$ . (b) Evolution of the panache distance with Richardson number for various values of temperature ratio  $\Lambda$ . ( $Pr = 0.71$  and  $Re = 586$ .)

in this section the initial velocity profile, at the nozzle exit, is taken uniform and parabolic.

In Fig. 11, we give the modified centerline velocity evolution  $U_{cm}$ , where  $U_{cm} = \frac{32U_c}{3(RiRe)^{0.5}}$ , for  $\Lambda = 0.75$  and for various Prandtl numbers  $Pr$ . It is noticed that, for small modified streamwise locations  $X_m$ , before  $X_m \approx 1$ , where  $X_m = RiX^2/Re$  measured from nozzle exit, this parameter is not influenced by Prandtl number and re-

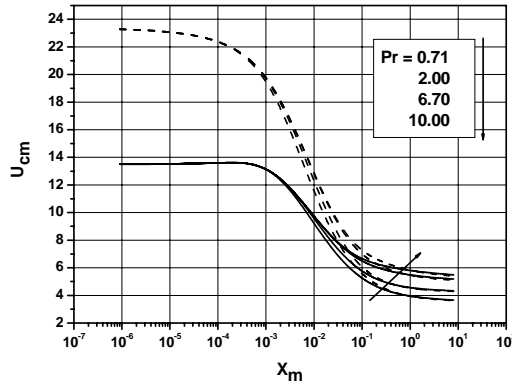


Figure 11: Evolution of the modified centerline streamwise velocity ( $U_{cm}$ ) of the jet influenced by Prandtl number (forced convection regime). (solid line: initial uniform profile, dashed line: initial parabolic profile,  $Ri = 5 \times 10^{-4}$  and  $\Lambda = 0.75$ ).

mains constant with value equal to the initial jet velocity. Indeed, in this region inertia forces dominate buoyancy forces and jet dynamic is mainly controlled by inertia forces. The jet behaves like a pure momentum source. We notice that the initial region, in which  $U_{cm}$  remains constant, doesn't exist when the initial velocity profile is taken to be parabolic as shown in Fig. 11. In fact, the modified centerline velocity decreases since the nozzle exit. This behavior is consistent with that found in [Fonade (1967)], suggesting that jet doesn't have potential core for this type of velocity profile. This result represents a first validation for our numerical model. For modified streamwise distances  $X_m > 1$ , far from the potential core, jet flow undergoes a velocity deceleration accompanied by a transverse enlargement, as in [Aissia, Zaouali, and Golli (2002)] for constant physical properties model. This phenomenon can be explained by an increase in the amount of surrounding fluid, which is initially at rest with  $U = 0$ , added to the jet flow by means of entrainment process. The entrainment process causes an augmentation in the mixing layer by shear, due to fluid viscosity, which develops on both sides of the potential core (only when the uniform initial velocity profile is used). We notice that the modified streamwise distance  $X_m$  from which the centerline velocity  $U_{cm}$  decreases depends slightly to Prandtl number as demonstrated by Fig. 11. Also, Fig. 11, suggests that in forced convection regime, defined for small Richardson numbers  $Ri = 5 \times 10^{-4}$ , buoyancy forces have significant effect only at very high modified streamwise distances  $X_m$  measured from the jet exit [Martynenko, Korovkin, and

Sokovishin (1989)]. The increase of this parameter, ie.  $U_{cm}$ , at these large stream-wise location  $X_m$ , is proportional to Prandtl number as suggests by [Martynenko, Korovkin, and Sokovishin (1989)].

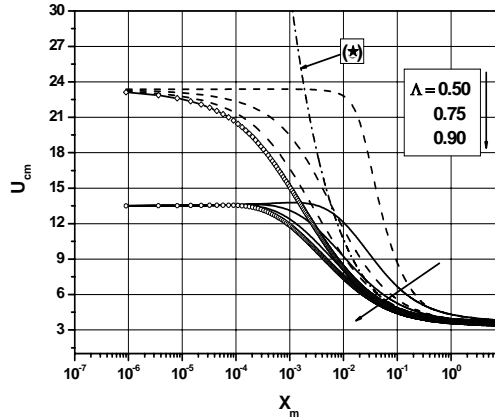


Figure 12: Evolution of the modified centerline streamwise velocity ( $U_{cm}$ ) of the jet compared with results obtained by [Martynenko, Korovkin, and Sokovishin (1989)](symbol :  $\star$ ) (forced convection regime). Effect of the parameter  $\Lambda$ . (solid line: initial uniform profile, dashed line: initial parabolic profile,  $Ri = 5 \times 10^{-4}$  and  $Pr = 0.71$ ).

In order to validate our numerical model, we compared the results obtained in the present study with those found by [Martynenko, Korovkin, and Sokovishin (1989)] who proposed analytical relations for both the centreline velocity and centreline temperature as a function of the Prandtl number. Indeed, it would be very important to find an analytical solution that is valid for arbitrary Prandtl numbers, but this implies great mathematical difficulties raised by the nonlinear character of the conservation equations Eq. 2. However, an approximate solution can be built. In fact, using as bases the results obtained for a Prandtl number equal to 2, and using the method of small perturbations, it is possible to obtain the centreline velocity,  $U_c$  and the centreline temperature  $\theta_c$ . These analytical equations show that for a given Richardson and Reynolds numbers, the effect of Prandtl number on the evolution of the centreline velocity and centreline temperature fields become more significant for increasing values of this parameter [for more details see Abbassi, Kechiche, and Aissia (2007) and Martynenko, Korovkin, and Sokovishin (1989)]. In this part we study the initial temperature ratio  $\Lambda$  influence on the jet dynamics.

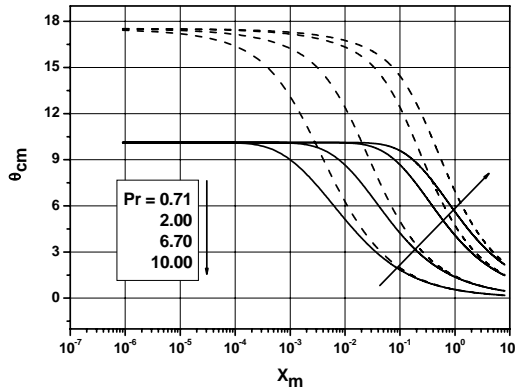


Figure 13: Evolution of the modified centerline temperature ( $\theta_{cm}$ ) of the jet influenced by Prandtl number (forced convection regime). (solid line: initial uniform profile, dashed line: initial parabolic profile,  $Ri = 5 \times 10^{-4}$  and  $\Lambda = 0.75$ ).

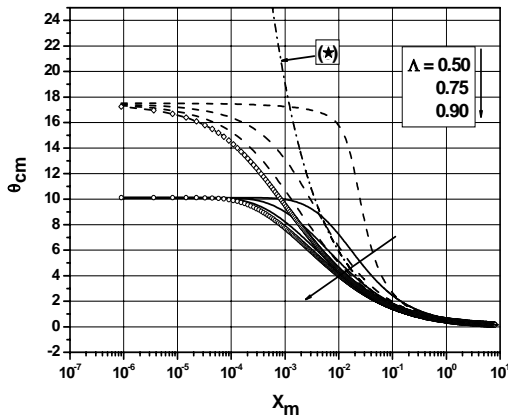


Figure 14: Evolution of the modified centerline temperature ( $\theta_{cm}$ ) of the jet compared with results obtained by [Martynenko, Korovkin, and Sokovishin (1989)] (symbol: ★) (forced convection regime). Effect of the by parameter  $\Lambda$ . (solid line: initial uniform profile, dashed line: initial parabolic profile,  $Ri = 5 \times 10^{-4}$  and  $Pr = 0.71$ ).

In Fig. 12, we presented results concerning the modified centerline velocity obtained by both mathematical models, variable and constant physical properties (standard model, symbol line (o)), compared with results given by [Martynenko, Korovkin, and Sokovishin (1989)] only in the region of interest (concerning forced convection) for high streamwise distance  $X$ . Indeed, the main goal of the comparison between the two mathematical models is to show how standard model results can be corrected when small temperature variation of physical properties is taken into consideration in the problem formulation. We notice that the same observations made for Prandtl number effect Fig. 11, concerning the jet characteristics, remain valid. However, it should be noted that the streamwise location  $X_m$  at which the modified centerline velocity decays is inversely proportional to the initial temperature ratio  $\Lambda$  proving a velocity acceleration of the jet. We are interested in forced convection regime in which analytical solutions proposed by [Martynenko, Korovkin, and Sokovishin (1989)] are available. Thereby, comparison between variable physical properties and analytical results obtained by [Martynenko, Korovkin, and Sokovishin (1989)] revealed excellent agreement in that region, defined by high distance  $X$ , where their solutions are valid [Abbassi, Kechiche, and Aissia (2007), Aissia, Zaouali, and Golli (2002)]. In Fig. 13, we traced the evolution of the modified centerline temperature  $\theta_{cm}$  according to the modified streamwise direction  $X_m$ . The evolution of the modified centerline temperature field, for  $Pr = 0.71$ , compared with that obtained by the standard model (symbol line (o)) and with analytical result proposed by [Martynenko, Korovkin, and Sokovishin (1989)] is depicted by Fig. 14. Also, we note an excellent agreement between results presented by [Martynenko, Korovkin, and Sokovishin (1989)] and our numerical results in the plume region defined by high streamwise distances  $X_m$  and characterized by negligible effect of inertia forces, which constitutes a good validation of the model presented herein. Note that the same observations still valid, although, we suggest that the mechanism which governs temperature field is more complicate than that of velocity. These differences will be discussed in more details in the last part.

### 3.3 Mixed convection regime

#### 3.3.1 Centerline velocity and temperature

In this last part we are interesting to the mixed convection regime characterized by domination of buoyancy forces compared to inertia forces. To achieve this goal we present an analysis of the hydrodynamic and thermal characteristics of the jet. For this purpose variable physical properties results are presented for Richardson number equal to 0.1 and for three values of the initial temperature ratio  $\Lambda$  ( $\Lambda = 0.5, 0.75$  and  $0.9$ ). The Prandtl number varies in the range  $0.71 \leq Pr \leq 10.00$ . In all results presented here both uniform and parabolic initial velocity profiles are used

and compared.

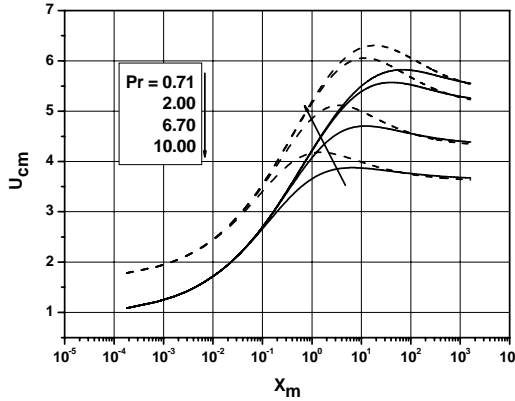


Figure 15: Evolution of the modified centerline streamwise velocity ( $U_{cm}$ ) of the jet influenced by Prandtl number (mixed convection regime). (solid line: initial uniform profile, dashed line: initial parabolic profile,  $Ri = 0.1$  and  $\Lambda = 0.75$ ).

In Fig. 15, we give the distribution of the modified centerline velocity  $U_{cm} = 32U_c/3 (Re Ri)^{0.5}$  as function of the modified streamwise distances  $X_m = Ri X^2 / Re$  measured from jet exit, for  $\Lambda = 0.75$  and for various Prandtl numbers  $Pr$ . With reference to Fig. 15, we notice that for small values of  $X_m$  ( $X_m < 10^{-3}$ ), the velocity profile have constant value like that found in forced convection regime (see §3.2.1). However, it's interested to note that the length of this region is less than that found in forced convection regime. This behaviour can be explained by an increased effect of buoyancy forces in the acceleration of centerline velocity  $U_{cm}$  of jet as explained by [Martynenko, Korovkin, and Sokovishin (1989), Abbassi, Kechiche, and Aissia (2007), Aissia, Zaouali, and Golli (2002)]. Also, it is obvious that Prandtl number effect is more felt in plume region defined by high streamwise distances  $X_m$  for both initial velocity profiles. This phenomenon has an important effect in the quality of heat transfer in the jet. This process will be analyzed by studying the effect of various parameters, such as  $Pr$  and  $\Lambda$ , on temperature field in the next paragraph.

The variable and constant physical properties (symbol line (o)) solutions of  $U_{cm} = 32U_c/3 (Re Ri)^{0.5}$  as function of the modified streamwise distances  $X_m = Ri X^2 / Re$ , for  $\Lambda = 0.5, 0.75$  and  $0.9$ , where they are compared with analytical solutions obtained by [Martynenko, Korovkin, and Sokovishin (1989)] is depicted by Fig. 16.

This figure confirms that, concerning the initial temperature ratio  $\Lambda$  effects, same observations made for Prandtl number (Fig. 15) remains valid. We notice that, for small value of  $X_m$  ( $X < 10^{-3}$ ), the difference between our numerical results and those presented by [Martynenko, Korovkin, and Sokovishin (1989)] is obvious because their analytical solutions are only valid in the plume region. However, for high streamwise locations  $X_m$  ( $X_m > 1$ , plume region) our results revealed excellent agreement with those of these authors [Martynenko, Korovkin, and Sokovishin (1989)]. In addition, comparison of solutions obtained by the present model with those obtained by the standard model shows that variation of physical properties with temperature increases the jet velocity along the center mainly in the plume region. By reference to Fig. 16, we also show that Prandtl number effect on hydrodynamic and heat transfer characteristics is only felt in the plume region, high  $X_m$  values, in which buoyancy term in the  $x$ -momentum equation Eq. 2 is not negligible. However, increases in the modified centerline velocity  $U_{cm}$  causes an inward flow in the opposite jet flow direction [Martynenko, Korovkin, and Sokovishin (1989)]. This behavior can be justified by an increase in the transverse velocity component  $V$ , by negative values, and an increase of jet expansion by entrainment phenomenon.

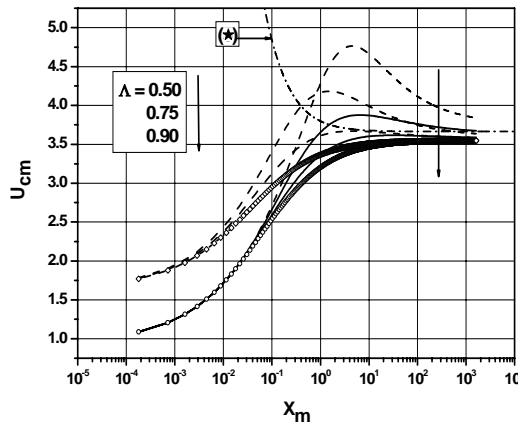


Figure 16: Evolution of the modified centerline streamwise velocity ( $U_{cm}$ ) of the jet compared with results obtained by [Martynenko, Korovkin, and Sokovishin (1989)](symbol:  $\star$ ) (mixed convection regime). Effect of the parameter  $\Lambda$ . (solid line: initial uniform profile, dashed line: initial parabolic profile,  $Ri = 0.1$  and  $Pr = 0.71$ ).

The modified centerline temperature profiles  $\theta_{cm}$  in mixed convection regime as function of the modified streamwise distances  $X_m = RiX^2/Re$ , for  $\Lambda = 0.75$ , and for various Prandtl number in the range ( $0.71 < Pr < 10$ ), is given by Fig. 17. We report in the same figure results obtained by the standard model and those given by [Martynenko, Korovkin, and Sokovishin (1989)]. We notice that analysis of the thermal field evolution is less obvious than that of the streamwise velocity field. Indeed, it is remarkable to note that the centerline temperature field evolution seems to be the result of complicate interaction between two phenomena with opposite effects. Firstly, increases in buoyancy term, high Richardson numbers, causes an increase in the streamwise velocity  $U_{cm}$  of the jet flow as shown in Fig. 15 and Fig. 16. Under this centerline velocity growth results an augmentation of the positive quantity of heat energy transferred in the same jet direction as explained by the stage in the temperature profile. Consequently, temperature of the jet increases. Secondly, the acceleration of the jet causes an augmentation in the amount of surrounding fluid incoming to jet flow caused by shear, due to fluid viscosity and explained by entrainment process. The growth of entrainment generates two effects. Indeed, on the one hand, we have a deceleration of jet explained by a decay in the centerline velocity, on the other hand, a negative fluid motion in the opposite direction of the flow characterized by a negative values in the transverse velocity profile. As a consequence of the entrainment growth is a negative quantity of heat energy transferred in the opposite direction of the flow causing a net decreases in

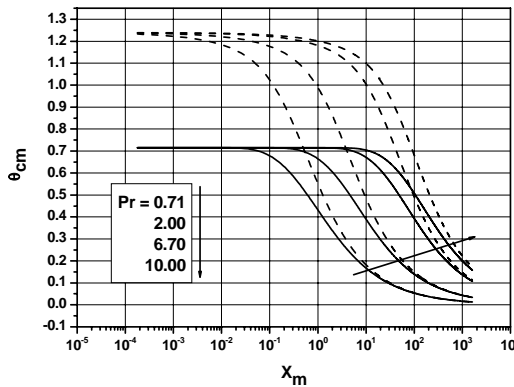


Figure 17: Evolution of the modified centerline temperature ( $\theta_{cm}$ ) of the jet influenced by Prandtl number (mixed convection regime). (solid line: initial uniform profile, dashed line: initial parabolic profile,  $Ri = 0.1$  and  $\Lambda = 0.75$ ).

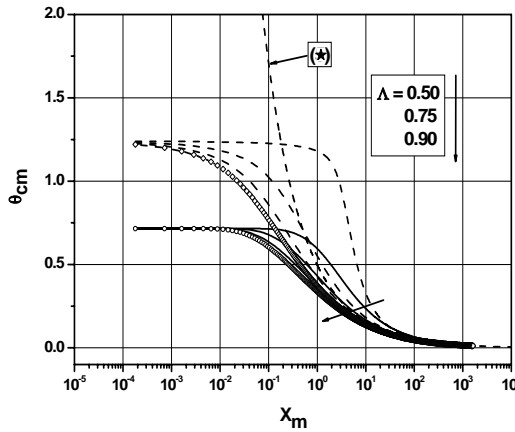


Figure 18: Evolution of the modified centerline temperature ( $\theta_{cm}$ ) of the jet compared with results obtained by [Martynenko, Korovkin, and Sokovishin (1989)](symbol:  $\star$ ) (mixed convection regime). Effect of the parameter  $\Lambda$ . (solid line: initial uniform profile, dashed line: initial parabolic profile,  $Ri = 0.1$  and  $Pr = 0.71$ ).

temperature of the jet [for more details of this phenomenon, see Abbassi, Kechiche, and Aissia (2007)]. It should be noted that this phenomenon increases with Prandtl number and decreases with initial temperature ratio  $\Lambda$ . Comparison between our results with those obtained by [Martynenko, Korovkin, and Sokovishin (1989)] shows good agreement in the plume region, defined by high streamwise distances  $X_m$ , where their analytic solutions are given, as shown in Fig. 18.

### 3.3.2 Dynamical and thermal half width

In Fig. 19, we represent, in mixed convection regime for Richardson number  $Ri = 0.1$ , the dynamical half-width  $Y_u^*$  and thermal half-width  $Y_\theta^*$  evolutions for various Prandtl number. Variable physical properties, for  $\Lambda = 0.5$  and  $\Lambda = 0.75$ , is compared with results obtained by the standard model (symbol line (o)). We notice that, in the plume region (high distances  $X$ ), the spreading of the jet is more important for small value of the initial temperature ratio parameter  $\Lambda$ . However, for small distances,  $X \leq 1$ , both  $Y_u^*$  and  $Y_\theta^*$  have constant value showing the existence of a potential core region, where buoyancy forces have negligible effects compared to inertia forces. It is also noted that the effect of Prandtl number is negligible in that region. For moderate streamwise distances  $X$  ( $1 \leq X \leq 10^2$ ) buoyancy and inertia

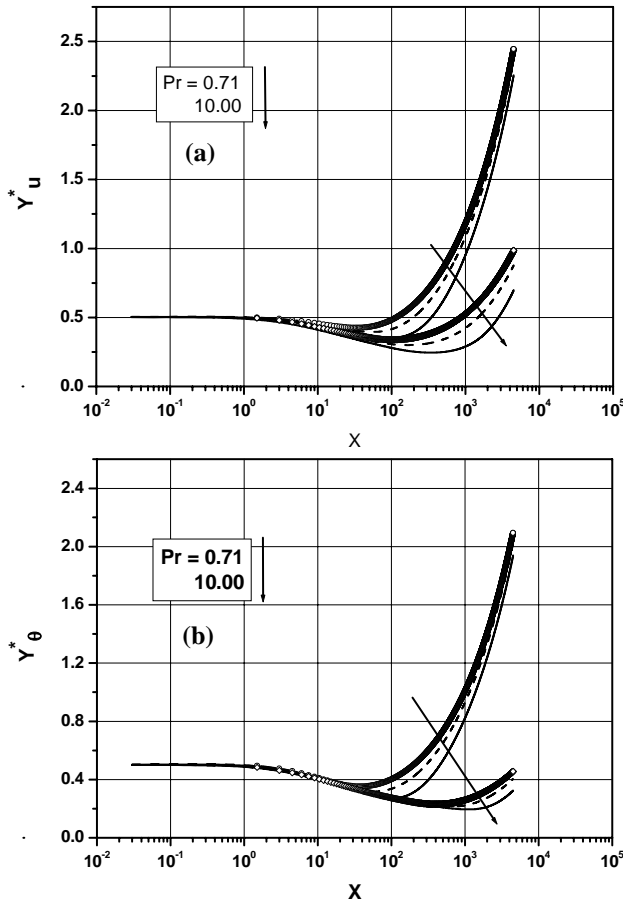


Figure 19: Effect of Prandtl number on dynamical and thermal half-widths (mixed convection regime). (a) Dynamical half-width  $Y_u^*$ . (b) Thermal half-width  $Y_\theta^*$ . (solid line:  $\Lambda = 0.50$ , dashed line:  $\Lambda = 0.75$ ,  $Ri = 0.1$ ).

forces become in the same order of magnitude, both  $Y_u^*$  and  $Y_\theta^*$  decrease, reach a minimum value and then increase again. With respect to Fig. 19a and Fig. 19b, we show that jet expansion undergoes a small reduction due to competition between two forces: buoyancy and inertia. For high streamwise distances  $X$  ( $X \geq 10^2$ ) jet behaviour is dominated by buoyancy forces as suggested by a rapid growth of  $Y_u^*$  and  $Y_\theta^*$ , respectively. This growth is inversely proportional to Prandtl number, but proportional to the initial temperature ratio  $\Lambda$  parameter. In addition, we notice that, for a given location  $X$ , the jet expansion is more significant for standard model than that for the present model as shown in both figures Fig. 19a and Fig. 19b.

## 4 Conclusions

In the present paper, we presented a numerical study of hydrodynamic and heat transfer characteristics of an incompressible steady and laminar round jet flow with variable physical properties influenced by Prandtl number. Both forced and mixed convection regimes are treated. In order to validate our numerical model, results are compared with those obtained analytically by [Martyntenko, Korovkin, and Sokovishin (1989)]. In the formulation of their work, these authors have not considered the dependence of physical properties with small heating rates, also they haven't taken into consideration the effects of the initial velocity profiles. In addition, comparison of results obtained in the present work are also made with those obtained numerically by standard model (constant physical properties).

The results obtained from numerical model presented in the present investigation show that both hydrodynamic and thermal fields are influenced by Prandtl number in both forced and mixed convection regions. It is important to note the existence of an entrainment phenomenon of the surrounding fluid into jet which is marked by a negative value of the transverse velocity component, which consistent subsequent works.

For the region close to jet exit, which is characterized by a low streamwise distances  $X$ , we notice that velocity and temperature fields are not affected by Prandtl number, and this is true for both forced and mixed convection regimes. However, results obtained by the present model show that initial velocity and temperature conditions have especially significant effects in that region (inertial region), where jet behaves like a pure momentum source. It should be noted that, in both forced and mixed convection regimes, the amount of surrounding fluid added to the jet by entrainment process increases with respect to the initial temperature ratio. At the vicinity of the jet exit, this entrainment have no effect on the quantity of heat energy transferred in the same direction as jet, resulting a stage in the temperature profile and a positive value of the transverse velocity component. However, at high longitudinal distance from the exit, the entrainment act in the opposite direction to the momentum diffusion, positive streamwise velocity component, marked by a negative value of transverse velocity; consequently temperature field of the jet decreases and the flow is cooled [Abbassi, Kechiche, and Aissia (2007)]. We also show that buoyancy forces act only at very high streamwise distances from the nozzle exit. The intensity of the buoyancy effect depends on Prandtl number value. However, the effect of buoyancy forces is more important in mixed convection regime, where the jet is accelerated with an expansion less than that in forced convection regime.

Comparison of our results with those obtained by [Martyntenko, Korovkin, and Sokovishin (1989)], who replace the emission conditions by considering two con-

straints of integration: conservation of momentum and energy to obtain analytical solutions valid only in the plume region, revealed an excellent agreement in that region for all Prandtl numbers used in the present work. This comparison proves reliability of the proposed model to predict global flow characteristics. Results are also compared with those obtained by classical model. The main effect of physical property variation with temperature is to increase the velocity of the jet with decreasing the expansion parameter.

## References

- Abbassi, A.; Kechiche, N.; Aissia, H. B.** (2007): Prandtl-number effects on vertical buoyant jets in forced and mixed convection regimes. *Energy conversion & management*, vol. 48, pp. 1435–1449.
- Aissia, H. B.; Zaouali, Y.; Golli, S. E.** (2002): Numerical study of the influence of dynamic and thermal exit conditions on axisymmetric laminar buoyant jet. *Numerical Heat Transfer, Part A*, vol. 42, pp. 427–444.
- Amielh, M.; Djeridane, T.; Anselmet, F.; Fulachier, L.** (1996): Velocity near-field of variable density turbulent jets. *International Journal of Heat and Mass Transfer*, vol. 39, no. 10, pp. 2149–2164.
- Boussinesq, J.** (1903): *Théorie Analytique de la Chaleur*. Vol. 2, Gauthier-Villars, Paris.
- Brown, W. B.; Donoughe, P. L.** (1951): *Tables of Exact Laminar Boundary Layer Solutions When the Wall is Porous and Fluid Properties are Variable*. NACA TN 2479.
- Chen, C. J.; Rodi, W.** (1980): *Vertical Turbulent Buoyant Jets a Review of Experimental Data*. Pergamon Press, Great Britain.
- Chua, L. P.; Antonia, R. A.** (1990): Turbulent Prandtl number in a circular jet. *International Journal of Heat and Mass Transfer*, vol. 33, pp. 331–339.
- Dalbert, A. M.; Penot, F.; Peube, J. L.** (1981): Convection naturelle laminaire dans un canal vertical chauffé à flux constant. *International Journal of Heat and Mass Transfer*, vol. 24, pp. 1463–1473.
- Fletcher, C. A. J.** (1991): *Computational techniques for fluid dynamics 1. Fundamental and general techniques*. Co. Springer-Verlag, Berlin Heidelberg, 2nd Ed.
- Fonade, C.** (1967): *Étude des jets. Application à la fluidique*. Institut national polytechnique de Toulouse.
- Gersten, K.** (1983): *Single-phase fluid flow, in Heat Exchanger Design Handbook*. Vol. 2 (Edited by E. U. Schlunder). Hemisphere, New York.

**Hirschfelder, J. P.; Curtiss, C. F.; Bird, R. B.** (1954): *Molecular Theory of Gases and Liquids*. J. Wiley and Sons, New York, NY.

**Kays, W. M.; Crawford, M. E.** (1980): *Convective heat and mass transfer*. Co. McGraw-Hill Book, New York, 2nd Ed.

**Kays, W. M.; Perkins, H. C.** (1973): *Forced convection, internal flow in ducts*. McGraw-Hill, New York.

**Kennard, E. M.** (1938): *Kinetic Theory of Gases*. McGraw Hill, New York.

**Landau, L. D.; Lifshitz, E. M.** (1943): *Fluid Mechanics*. Pergamon Press, Oxford.

**Martynenko, O. G.; Korovkin, V. N.; Sokovishin, Y. A.** (1989): The class of self-similar solutions for laminar buoyant jets. *Int. J. Heat Mass Tran.*, vol. 32, pp. 2297–2307.

**Panchapakesan, N. R.; Lumley, J. L.** (1993): Turbulence measurements in axisymmetric jets of air and helium. Part 2. Helium jet. *Journal of Fluid Mechanics*, vol. 246, pp. 225–247.

**Peterson, J.; Bayazitoglu, Y.** (1992): Measurements of velocity and turbulence in vertical axisymmetric isothermal and buoyant jets. *Journal of Heat Transfer*, vol. 114, pp. 135–142.

**Svehla, R. A.** (1962): *Estimated Viscosities and Thermal Conductivities of Gases at High Temperatures*. NASA Technical Report R132.

**Yassine, Z.; Aissia, H. B.; Kechiche, N.; Jay, J.; Schon, J. P.** (2004): Experimental study of the instabilities in the laminar turbulent transition zone of an axisymmetric jet at low Reynolds numbers. *Journal of Flow Visualization & Image Processing*, vol. 11, pp. 1–16.

